

## Semiclassical theory of two-photon induced Raman scattering

W. H. Louisell\* and P. Meystre

*Max Planck Gesellschaft zur Förderung der Wissenschaften e. V., Projektgruppe für Laserforschung, D-8046 Garching, Federal Republic of Germany*

(Received 1 July 1980)

Stimulated two-photon induced Raman scattering (hyper-Raman scattering) in an amplifier consisting of four-level atoms is analyzed semiclassically, via the coupled density matrix and Maxwell equations. We consider conditions typically encountered in the optical regime and in vapors. We show that even in the linear regime, it is characterized by a significant depletion of the atomic ground-state population, thus invalidating perturbative analyses based, for instance, on the nonlinear susceptibility tensor. Two major regimes of operation are found, one in which the population is completely consumed by the interaction ("linear regime"), and one in which the pump laser is depleted ("nonlinear regime"). Both regimes are, however, characterized by small photon conversion efficiencies. The tuning range is also briefly discussed.

### I. INTRODUCTION

In recent years, the study of higher order nonlinear optical processes has been the object of much activity,<sup>1</sup> both theoretically and experimentally. In general, it is argued that in the small signal regime, it is sufficient to describe these effects perturbatively, for instance via a nonlinear susceptibility. In the case of Raman scattering, in particular, this approach has been very successful at predicting the output power of the system.

Recently, Reif and Walther<sup>2</sup> have used two-photon induced Raman scattering in a four-level system (strontium vapor) to produce 16- $\mu\text{m}$  radiation, and found a series of results which are at odds with conventional perturbative treatments using nonlinear susceptibilities. The most striking of these is that the output versus input power does not follow an  $\exp(I_L^2 z)$  growth, where  $I_L$  is the laser pump power and  $z$  the distance. They note, however, that "the photon conversion efficiency... is far from creating ground-state depletion which leads to saturation effects." This would imply that this experiment was indeed performed in the small signal regime. This is a reasonable assumption, since a two-photon transition was involved in the pumping cycle. It is, however, important to note that the output value of the driving field was not measured.

In this same experiment, the tuning characteristics of the system were measured, and it was shown to be nonsymmetrical, with a dip near line center. The presence of the dip, which did not appear in a different vapor considered by Hanna *et al.*,<sup>3</sup> was attributed to competing processes, but the effects of the hyper-Raman process itself were not singled out.

In more recent experiments,<sup>4</sup> the spectrum of the 16- $\mu\text{m}$  radiation was measured, and it does

not seem to agree with what would be expected from a simple-minded extrapolation of the Raman scattering results.

The major discrepancies between experimental results and a perturbation analysis justify restudying hyper-Raman scattering in four-level systems, and trying to determine the causes of the disagreement.

In this paper, we present a theory of this effect starting from first principles. We describe the fields classically and the medium quantum mechanically via its density matrix. In Sec. II, we give the formal development of the theory. We perform the slowly varying amplitude and phase approximation, together with the rotating wave approximation. We neglect the coupling with the backward propagating waves. This is justified, provided that both the Stokes and idler wave amplitudes remain small. We then obtain the equations of motion for the elements of the density matrix and the fields.

Even in the limit where the atoms follow the fields adiabatically,<sup>5</sup> the (now algebraic) density matrix equations are extremely complex. It is, however, easy to convince oneself that it is inconsistent, even in a linearized theory, to neglect the depletion of the ground level. This is analogous to a situation which has previously been encountered, albeit under very particular conditions, in usual Raman scattering.<sup>6</sup>

In Sec. III we solve numerically the coupled density matrix and Maxwell equations. We show that indeed, the population of the ground level is significantly depleted, even though the Stokes signal remains extremely small. We distinguish between two types of saturation, due, respectively, to the depletion of the number of active atoms and to the depletion of the pump.

In the first case, the pump field is practically not depleted. This would usually be called the

small-signal (or linear) regime. In hyper-Raman scattering, it is, however, characterized by a strong saturation of the medium. Clearly, since in this regime all the atoms are used up, an increase of the pump does not result in any increase of the Stokes field.

The other type of saturation (depletion of the pump field) is likewise *not* characterized by a large Stokes field. This is due to the fact that, contrary to what happens in Raman scattering, there are other channels of interaction than those leading to amplification. Thus, a small Stokes field does not imply at all that one is in the linear regime. We have computed the output intensity versus input intensity in this regime, and find a good qualitative agreement with the results of Reif and Walther. Thus, we argue that in this experiment the pump field was significantly depleted.

We conclude this section by computing the tuning curve of the system, and find that it is nonsymmetrical about the line center. This is in qualitative agreement with the experimental results of Hanna *et al.*<sup>3</sup> Note that our approach is quite different from that of Ref. 5, where no self-consistent solution of the problem was derived. Rather, the polarization driving the Stokes field was evaluated numerically at steady state, for fixed values of the Stokes and/or driving fields, and for various detunings.

Finally, Sec. IV is a summary and conclusion. Some remarks on the numerical technique used are presented in Appendix A. The discussion of the spectrum will be the subject of a future publication.

## II. FORMAL DEVELOPMENT

In Fig. 1 we show the four-level atomic scheme relevant for two-photon near resonant stimulated hyper-Raman scattering theory. We consider a homogeneously broadened medium. The pump, Stokes, and idler frequencies are  $\omega_L$ ,  $\omega_S$ , and  $\omega_I$ , respectively. The detunings are  $\Delta_1$  and  $\Delta_2$ , where

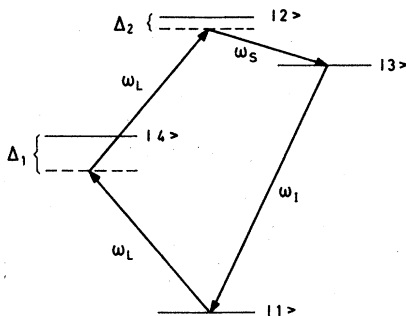


FIG. 1. Four-level system, with the detunings  $\Delta_1$  and  $\Delta_2$ , and the frequencies  $\omega_L$  (laser),  $\omega_S$  (Stokes), and  $\omega_I$  (idler).

one usually has  $\Delta_1 \gg \Delta_2$ . Selection rules allow transitions between levels 1 and 4, 2 and 4, 2 and 3, and 3 and 1. This is different from the model of Ref. 5, where this last transition was not considered. As noted in the Introduction, we may neglect the backward traveling Stokes and idler waves, provided that their amplitudes always remain small. We will see *a posteriori* that this is justified under the conditions considered here.

We consider the case where the two-photon excitation is produced by a single laser. We assume that the fields are plane polarized and given by

$$E(z, t) = \sum_{i=1}^3 E_i(z, t) \cos \zeta_i, \quad (2.1)$$

where

$$\zeta_i = k_i z - \omega_i t + \varphi_i(z, t). \quad (2.2)$$

The  $i = 1$  term refers to the pump,  $i = 2$  is the Stokes, and  $i = 3$  is the idler. We also assume perfect phase matching and let

$$\omega_L = ck_L, \quad \omega_S = ck_S, \quad \omega_I = 2\omega_L - \omega_S = ck_I. \quad (2.3)$$

The amplitudes  $E_i$  and phases  $\varphi_i$  are assumed to be slowly varying.

The polarization is of the form

$$\rho(z, t) = \sum_{i=1}^3 [C_i(z, t) \cos \zeta_i + S_i(z, t) \sin \zeta_i], \quad (2.4)$$

and is explicitly given by

$$\rho(z, t) = N \text{Tr}(\zeta \mu), \quad (2.5)$$

where  $\zeta$  is the density matrix describing the system and  $N$  is the atomic number density. (We use mks units.)

Since only forward waves are considered, it is convenient to introduce the retarded time

$$\tau = t - z/c; \quad z' = z. \quad (2.6)$$

The field and polarization may then be written

$$E(z, t) = \bar{E}(z', \tau) = \frac{1}{2} \sum_i (\delta_i e^{-i\omega_i \tau} + \text{c.c.}), \quad (2.7)$$

$$P(z, t) = \bar{P}(z', \tau) = -\frac{i}{2} \sum_i (\mathcal{P}_i e^{-i\omega_i \tau} + \text{c.c.}), \quad (2.8)$$

where

$$\delta_i = \bar{E}_i(z', \tau) \exp[i\bar{\varphi}_i(z', \tau)], \quad (2.9a)$$

$$\mathcal{P}_i = [\bar{C}_i(z', \tau) + i\bar{S}_i(z', \tau)] \exp[i\bar{\varphi}_i(z', \tau)]. \quad (2.9b)$$

Under the slowly varying amplitude and phase approximation, Maxwell's equations reduce to

$$(\partial/\partial z' + \kappa_i/2)\delta_i = k_i \mathcal{P}_i/2\epsilon_0. \quad (2.10)$$

The  $\kappa_i$  represent phenomenological linear losses.

To obtain the slowly varying parts of the density matrix, we let

$$\begin{aligned} \rho_{12} &= \bar{\rho}_{12} \exp(2i\omega_L \tau); & \rho_{23} &= \bar{\rho}_{23} \exp(-i\omega_S \tau), \\ \rho_{13} &= \bar{\rho}_{13} \exp(i\omega_I \tau); & \rho_{24} &= \bar{\rho}_{24} \exp(-i\omega_L \tau), \\ \rho_{14} &= \bar{\rho}_{14} \exp(i\omega_L \tau); & \rho_{34} &= \bar{\rho}_{34} \exp[i(\omega_S - \omega_L)\tau]. \end{aligned} \quad (2.11)$$

The polarization (2.8) then becomes

$$\begin{aligned} \bar{P}(z', \tau) = N[ & (\mu_{14}\bar{\rho}_{41} + \mu_{42}\bar{\rho}_{24}) \exp(-i\omega_L\tau) \\ & + \mu_{32}\bar{\rho}_{23} \exp(-i\omega_s\tau) + \mu_{13}\bar{\rho}_{31} \exp(-i\omega_I\tau) + \text{c.c.}] \end{aligned} \quad (2.12)$$

The first two terms give the pump polarization. They do not change much in the linear undepleted pump regime. (Note, however, that we shall also consider the general case where the pump is significantly depleted.) The third term is the polarization generated at the Stokes frequency and the fourth is the idler polarization.

With the ansatz (2.12) and the rotating wave approximation, the diagonal density matrix equations reduce to

$$\frac{\partial \rho_{11}}{\partial \tau} = \gamma_{44}\rho_{44} + \gamma_{33}\rho_{33} + i(\mu'_{14}\bar{\rho}_{41}\mathcal{E}_L^* + \mu'_{13}\bar{\rho}_{31}\mathcal{E}_I^* - \text{c.c.}), \quad (2.13)$$

$$\frac{\partial \rho_{22}}{\partial \tau} = -\gamma_{22}\rho_{22} + i(\mu'_{24}\bar{\rho}_{42}\mathcal{E}_L + \mu'_{23}\bar{\rho}_{32}\mathcal{E}_s - \text{c.c.}), \quad (2.14)$$

$$\frac{\partial \rho_{33}}{\partial \tau} = \beta\gamma_{22}\rho_{22} - \gamma_{33}\rho_{33} + i(\mu'_{32}\bar{\rho}_{23}\mathcal{E}_s^* + \mu'_{31}\bar{\rho}_{13}\mathcal{E}_I - \text{c.c.}), \quad (2.15)$$

$$\frac{\partial \rho_{44}}{\partial \tau} = (1-\beta)\gamma_{22}\rho_{22} - \gamma_{44}\rho_{44} + i(\mu'_{41}\bar{\rho}_{41}\mathcal{E}_L + \mu'_{42}\bar{\rho}_{24}\mathcal{E}_L^* - \text{c.c.}). \quad (2.16)$$

Here,  $\beta$  is a branching ratio giving the relative probabilities of spontaneous decay of level 3 into 2 and 4, respectively.

It follows that

$$\text{Tr}\rho = 1, \quad (2.17)$$

which merely expresses the fact that we are considering a closed atomic system. The conservation of energy relation (2.17) can be used as one check on the computer results. We have let

$$\mu'_{ij} \equiv \mu_{ij}/2\hbar. \quad (2.18)$$

From (2.13)–(2.16) one can see that in a linear theory in  $\mathcal{E}_s$  and  $\mathcal{E}_I$ , we should expect the population of level 3 to be much smaller than that of the other levels, since the pump amplitude does not appear explicitly.

The off-diagonal density matrix equations reduce to

$$\begin{aligned} \frac{\partial \bar{\rho}_{21}}{\partial \tau} = & -(i\Delta_2 + \gamma_{21})\bar{\rho}_{21} + i(\mu'_{24}\bar{\rho}_{41}\mathcal{E}_L - \mu'_{41}\bar{\rho}_{24}\mathcal{E}_L \\ & + \mu'_{23}\bar{\rho}_{31}\mathcal{E}_s - \mu'_{31}\bar{\rho}_{23}\mathcal{E}_I), \end{aligned} \quad (2.19)$$

$$\frac{\partial \bar{\rho}_{13}}{\partial \tau} = -\gamma_{13}\bar{\rho}_{13} + i[\mu'_{14}\bar{\rho}_{43}\mathcal{E}_L^* - \mu'_{13}(\rho_{11} - \rho_{33})\mathcal{E}_I^* - \mu'_{23}\bar{\rho}_{12}\mathcal{E}_s], \quad (2.20)$$

$$\begin{aligned} \frac{\partial \bar{\rho}_{41}}{\partial \tau} = & -(i\Delta_1 + \gamma_{41})\bar{\rho}_{41} + i[\mu'_{41}(\rho_{11} - \rho_{44})\mathcal{E}_L \\ & + \mu'_{42}\bar{\rho}_{21}\mathcal{E}_L^* - \mu'_{31}\bar{\rho}_{43}\mathcal{E}_I], \end{aligned} \quad (2.21)$$

$$\begin{aligned} \frac{\partial \bar{\rho}_{23}}{\partial \tau} = & -(i\Delta_2 + \gamma_{23})\bar{\rho}_{23} + i[\mu'_{24}\bar{\rho}_{43}\mathcal{E}_L \\ & - \mu'_{23}(\rho_{22} - \rho_{33})\mathcal{E}_s - \mu'_{13}\bar{\rho}_{21}\mathcal{E}_I^*], \end{aligned} \quad (2.22)$$

$$\begin{aligned} \frac{\partial \bar{\rho}_{24}}{\partial \tau} = & -[i(\Delta_2 - \Delta_1) + \gamma_{24}]\bar{\rho}_{24} + i[\mu'_{14}\bar{\rho}_{21}\mathcal{E}_L^* + \mu'_{24}(\rho_{22} - \rho_{44})\mathcal{E}_L \\ & - \mu'_{23}\bar{\rho}_{34}\mathcal{E}_s], \end{aligned} \quad (2.23)$$

$$\begin{aligned} \frac{\partial \bar{\rho}_{43}}{\partial \tau} = & -(i\Delta_1 + \gamma_{43})\bar{\rho}_{43} + i(\mu'_{41}\bar{\rho}_{13}\mathcal{E}_L + \mu'_{42}\bar{\rho}_{23}\mathcal{E}_L^* \\ & - \mu'_{13}\bar{\rho}_{41}\mathcal{E}_I^* - \mu'_{23}\bar{\rho}_{42}\mathcal{E}_s), \end{aligned} \quad (2.24)$$

together with their complex conjugates. In a linear theory it would be consistent to take  $\rho_{33} \simeq 0$ , as can be seen from (2.15), (2.20), and (2.22), so that

$$\rho_{11} + \rho_{22} + \rho_{44} \simeq 1. \quad (2.25)$$

By (2.15) we see that

$$\mu'_{32}\bar{\rho}_{23}\mathcal{E}_s + \mu'_{31}\bar{\rho}_{13}\mathcal{E}_I - \text{c.c.} \simeq 0. \quad (2.26)$$

This still leaves so many equations that one cannot do much analytically. By inspection of the density matrix equations it is easy to convince oneself that it is *a priori* inconsistent, even in the linear, quasi-cw regime, to neglect the populations of the upper levels (except for level 3, as already discussed). The reason is very simple, namely that  $\rho_{22}$  and  $\rho_{44}$  appear together with  $\mathcal{E}_L$ . When inspecting how these terms propagate through the equations, one sees that in the best case (that is, assuming  $\mathcal{E}_I$  and  $\mathcal{E}_s$  very small), they are still of the same order as terms linear in  $\mathcal{E}_s$  or  $\mathcal{E}_I$ . Since one can obviously not neglect these last terms if one wants to obtain any gain at all, it is therefore inconsistent to neglect the populations of levels 2 and 4. As we shall see in Sec. III, this is fully confirmed numerically. We find not only that we cannot ignore  $\rho_{22}$  and  $\rho_{44}$ , but also that the population of the ground level is always significantly depleted.

### III. STOKES INTENSITY

In this section, we present the results of the numerical solution of the coupled density matrix and Maxwell equations. Some comments on the numerical method are given in Appendix A. For convenience, the fields are expressed in terms of Rabi frequencies  $\Omega_L$ ,  $\Omega_s$ , and  $\Omega_I$ . This can be done without ambiguity for the Stokes and idler fields

$$\begin{aligned} \Omega_s &= \mu_{23}\mathcal{E}_s/2\hbar, \\ \Omega_I &= \mu_{31}\mathcal{E}_I/2\hbar. \end{aligned} \quad (3.1)$$

However, the pump field appears in (2.19) with

the two dipole moments  $\mu_{41}$  and  $\mu_{24}$ . We have chosen to express it in terms of the Rabi frequency

$$\Omega_L = \mu_{41} \mathcal{E}_L / 2\hbar, \quad (3.2)$$

so that a factor  $\mu_{24}/\mu_{41}$  must be introduced in expressions containing  $\mu_{24} \mathcal{E}_L$ .

The incident driving field is taken to be real and Gaussian:

$$\Omega_L(0, \tau) = \Omega_0 \exp[-(\tau - \tau_0)^2 / \bar{\tau}^2], \quad (3.3)$$

and the initial Stokes and idler fields are taken as small constants. This implies that we describe the amplification of small initial Stokes and idler waves. If we were to discuss the buildup from noise, the initial polarization would have to be taken as random noise in this semiclassical approach.

In terms of Rabi frequencies, the field equations become

$$\begin{aligned} \left( \frac{\partial}{\partial z'} + \kappa_L/2 \right) \Omega_L &= iak_L (|\mu_{14}|^2 \bar{\rho}_{41} + \mu_{41} \mu_{42} \bar{\rho}_{24}), \\ \left( \frac{\partial}{\partial z'} + \kappa_S/2 \right) \Omega_S &= iak_S |\mu_{23}|^2 \bar{\rho}_{23}, \\ \left( \frac{\partial}{\partial z'} + \kappa_I/2 \right) \Omega_I &= iak_I |\mu_{13}|^2 \bar{\rho}_{31}, \end{aligned} \quad (3.4)$$

where

$$a = N/2\hbar\epsilon_0.$$

Expressing the dipole moments  $|\mu_{ij}|^2$  in terms of the corresponding Einstein  $A_{ij}$  coefficients<sup>7</sup>

$$|\mu_{ij}|^2 = 3\pi\hbar\epsilon_0/\tau_{ij} k_{ij}^3, \quad (3.5)$$

we can re-express (3.4) as

$$\begin{aligned} \left( \frac{\partial}{\partial z'} + \kappa_L/2 \right) \Omega_L &\approx i(N_{\text{eff}}/\omega_L^2) [\bar{\rho}_{41}/\tau_{41} + (\mu_{41}/\mu_{24})(\bar{\rho}_{24}/\tau_{42})], \\ \left( \frac{\partial}{\partial z'} + \kappa_S/2 \right) \Omega_S &\approx i(N_{\text{eff}}/\omega_S^2) (\bar{\rho}_{23}/\tau_{23}), \\ \left( \frac{\partial}{\partial z'} + \kappa_I/2 \right) \Omega_I &\approx i(N_{\text{eff}}/\omega_I^2) (\bar{\rho}_{31}/\tau_{13}), \end{aligned} \quad (3.6)$$

where  $N_{\text{eff}} = (3\pi Nc^2/2)$  acts as an effective "density."

We still have to relate the Einstein coefficients to the decay rates of the diagonal elements of the density matrix. If we consider a closed four-level system, this presents no ambiguity for levels 3 and 4. However, for level 2, we must introduce the branching ratio  $\beta$  giving the relative probabilities of spontaneous decay to the levels 3 and 4.

We take the atomic system to be initially in its ground state, so that

$$\rho_{11}(z', 0) = 1 \quad (3.7)$$

and

$$\begin{aligned} \rho_{ii}(z', 0) &= 0, \quad i \neq 1 \\ \rho_{ij}(z', 0) &= 0, \quad i \neq j. \end{aligned} \quad (3.8)$$

This completes the preparation for the numerical analysis.

#### A. Output intensity

In the results that we shall discuss first, the following values have been chosen for the various parameters: The decay rates of the populations of levels 2, 3, and 4 are  $\gamma_{22} = 1$ ,  $\gamma_{33} = 1$ , and  $\gamma_{44} = 0.5$ , respectively. The dephasing rates are all taken to be the same,  $\gamma_{ij} = 10$ . This is a good approximation for a pressure broadened system. The branching ratio  $\beta$  is taken to be  $\frac{1}{2}$ , and the pump pulse duration = 0.5, in units of  $1/\gamma_{22}$ . We assume the dipole moments  $\mu_{14}$  and  $\mu_{24}$  to be the same. Finally,  $\kappa_i = 0$ , and the frequencies of the laser, stokes, and idler fields, respectively, are in the ratio 1.75 : 1 : 2.5. The coefficient  $N_{\text{eff}}/\omega_L^2$  is taken to be  $\sim 51.0$ . The detunings are  $\Delta_1 = 10$  and  $\Delta_2 = 1$ , in units of  $\gamma_{22}$ .

This set of values is reasonable for typical experiments in vapors (although the detunings considered here are much smaller than those of Ref. 2). They indicate that it is *a priori* doubtful that a nonlinear susceptibility approach would give satisfactory results in vapor experiments, since the expression for  $\chi^{(5)}$  is based on an adiabatic elimination of the material variables. This approximation is far from being justified for the set of values that we are considering. (In liquids or solids, however, the medium relaxation times are normally much shorter than the pump pulse duration. Thus, the results discussed here cannot be readily generalized to that case, where the dynamics occurs on completely different time-scales). We finally note that our choice of parameters presents the advantage of yielding similar growth rates for all fields, thus simplifying the choice of a grid for the numerical time integration.

In Fig. 2, we present the output Stokes intensity as a function of the length of the amplifier for various values of the peak pump field. The pulse duration and detuning are kept constant.

We first note that for a small amplifier length, the growth of the Stokes field is independent of the incident power. Except for very short  $z$ , it is essentially exponential. This is surprising, since one would intuitively expect it to be strongly power dependent ( $I_L^2$ ). This clearly indicates that the growth is not governed by the pump, but rather is limited by the number of atoms present in the amplifier. This is confirmed by looking at the diagonal elements of the density matrix, which are shown in Fig. 3 for fixed  $z$  and various pump powers as a function of the retarded time  $\tau$ . We see that

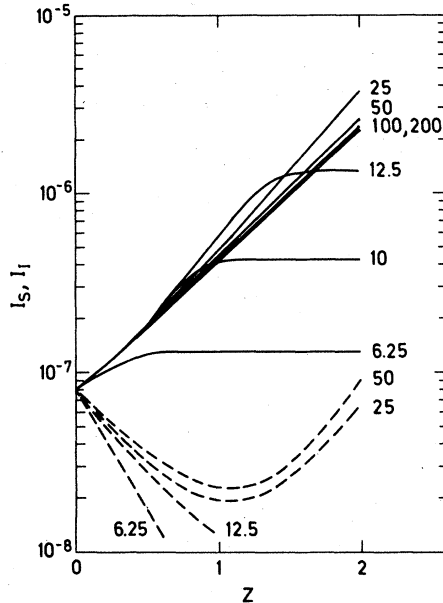


FIG. 2. Stokes energy (solid lines) and idler energy (dashed lines) as a function of amplifier length (arbitrary units). The numbers label the peak Rabi frequency of the driving field, which is taken to be Gaussian of width  $\frac{1}{2}$ , in units of  $\gamma_{22}$ . The atomic relaxation times are  $\gamma_{22}=1$ ,  $\gamma_{33}=1$ , and  $\gamma_{44}=\frac{1}{2}$ . The polarization decay time is  $\gamma=10$ , and the detunings are  $\Delta_2=1$  and  $\Delta_1=10$ . The field frequencies are in the ratio  $\omega_L:\omega_S:\omega_I=1.75:1:2.5$ , and  $N_{\text{eff}}/\omega_L^2=51$ . The linear losses are taken to be zero.

when the driving field reaches its maximum, the atomic system is completely saturated, and the populations of levels 1, 2, and 4 are all about equal to  $\frac{1}{3}$ . For strong pump fields, there is a significant pulsation of the populations of the various levels, which, however, disappears for weaker driving fields. (note, however, that the population of level 3 remains always small, as indicated in Sec. II).

A similar situation is also possible in usual Raman scattering.<sup>6</sup> If, for instance, the upper level can also be ionized, instead of only being allowed to decay, then the growth rate of the Stokes field can become independent of the pump power, in the linear regime. Although the physics underlying this problem and two-photon induced Raman scattering is different, the basic reason why this can happen is the same in both cases, namely the presence of competing processes. For hyper-Raman scattering, and in the absence of an idler wave, they have been identified as "laser" (or one-photon) and "Raman" (or two-photon) terms.<sup>5</sup> In our case, the presence of an idler field leads to a further complication, since four-wave parametric processes are also possible. They can play an important role here, since we assume exact phase matching. (See also Ref. 1, p. 241.)

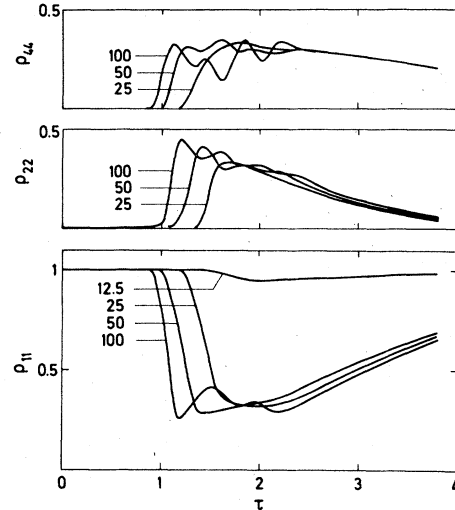


FIG. 3. Population of the levels 1, 2, and 4 as a function of the retarded time  $\tau$  for a fixed position in the amplifier ( $z=1.8$  in the units of Fig. 2). The time is in units of  $1/\gamma_{22}$ . The numbers label the peak Rabi frequency of the input laser field, which has the same temporal behavior as in Fig. 2, and peaks at  $\tau=1.5$ . The other parameters are the same as in Fig. 2.

That one should obtain a significant population of the upper levels 2 and 4 is rather surprising, since the excitation is produced by a two-photon process. Intuitively, one would expect the atoms to remain essentially in the ground state. One could object that this is a "spurious" effect, due to the fact that we have considered unreasonably small detunings in comparison with the Rabi frequency of the driving field. In Sec. III B we shall discuss this point in more detail and show that the Rabi frequency is not a good parameter in this problem.

As the amplifier length is increased, the Stokes power corresponding to low input fields starts to saturate. This is due to the depletion of the pump, which occurs obviously sooner for lower inputs. We observe that before the onset of saturation, the growth of the Stokes field per unit length first increases slightly. We attribute this feature to the combined effects of the atoms not being strongly saturated any more, together with polarizations still large enough to produce significant amplification. In other words, the competing processes become relatively less important, compared to the Stokes amplification. This is illustrated in Fig. 3, where we see that near the onset of saturation of the Stokes field ( $\Omega_L=25$ ), the pulsations of the atomic population disappear. For this short length of amplifier, then, the system tries to behave as in the "true" small-signal regime.

The pump energy as a function of amplifier length

is shown in Fig. 4. Two points are worth noting about these curves. First, the energy lost by the pump laser when the medium is completely saturated is always the same, within the accuracy of the numerical integration. However, the depletion becomes highly pump dependent when the Stokes output is saturated. This is, of course, consistent with the interpretation that in the first regime, the maximum amount of energy which can be extracted depends only upon the available atoms, while when the Stokes output saturates, the atomic medium ceases to be saturated and the pump depletion must depend upon its initial amplitude.

The second point is that the output Stokes is always only a small fraction of the initial pump power. This also may appear surprising, since one would expect that when the depletion of the pump is significant, a considerable amount of energy is transferred to the Stokes (or idler) field. This, however, does not hold for hyper-Raman scattering, because of the lower order competing processes which use up most of the input energy. This point will be discussed in more detail in Secs. IIIB and IIIC.

We now turn to a brief discussion of the idler field. As is shown in Fig. 2,  $I_s$  first decreases, before following a growth pattern very much like that of the Stokes wave. The initial absorption is due to the fact that the population of level 3 always remains very small. Thus, the atoms act as a very effective absorber at the idler wavelength.

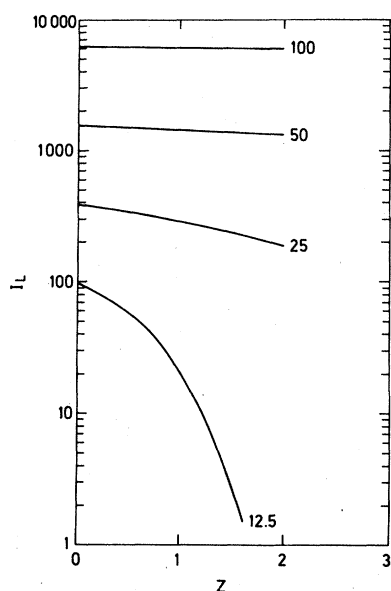


FIG. 4. Energy of the laser field as a function of amplifier length (arbitrary units). The parameters are the same as in Fig. 2. The numbers label the peak Rabi frequency of the input laser field.

One may wonder if the saturation of the material could not be avoided simply by increasing the atomic density. By simple inspection of Maxwell's equations, however, it is easy to convince oneself that this is equivalent to rescaling the amplifier length. Thus, the only change will be the values of the pump fields at which depletion takes over, but the basic physics remains the same.

It is interesting to note that although the Stokes energy remains constant in the "small-signal regime," the pulse shape is different for various peak powers of the driving field. This is illustrated in Fig. 5, where we observe the appearance of a shoulder and a slight broadening of the Stokes pulse for increasing incident powers.

#### B. Effects of detuning

As already mentioned, the question remains to determine to which extent the results discussed up to now are due to the relatively small detunings that we have considered. In Fig. 6, we present the output Stokes intensity as a function of amplifier length under the same conditions as in Fig. 2, but for a detuning  $\Delta_1 = 100$ . We see that the results are qualitatively the same, with, however, an important difference: The transition from the regime where the medium is completely saturated to that where the field is depleted is much slower. As a consequence, there is a range of incident fields for which one obtains a larger output for a larger detuning. In this same region, and for a fixed detuning, one obtains a larger output for smaller driving fields. Again, we attribute this rather remarkable result (which was also apparent, although much weaker, in Fig. 2) to the fact that in that last case, it is harder to saturate the upper levels 2 and 4. Thus, the role of the "laser"

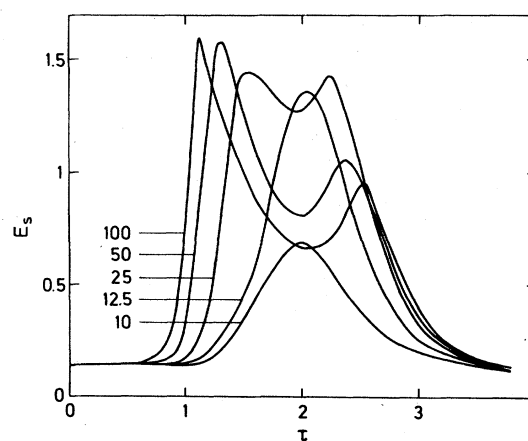


FIG. 5. Pulse shape of the output Stokes field for a fixed amplifier length and various peak input laser Rabi frequencies. The input field peaks at  $\tau = 1.5$ . (Retarded time in units of  $1/\gamma_{22}$ , parameters same as in Fig. 2.)

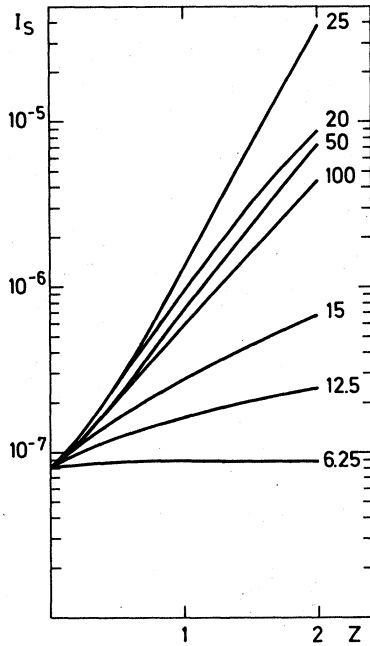


FIG. 6. Same as Fig. 2, but for  $\Delta_1 = 100$ .

and "Raman" effects become relatively less important compared to hyper-Raman scattering.

It is worth mentioning that for the large detunings considered here, we still obtain a significant depletion of the ground level. For  $\Delta_1 = 100$  and an incident peak power as small as 25, for instance we find that less than 40% of the population is left in level 1 at the peak of the pump pulse. This is surprising in view of the small Rabi frequency compared to the detuning  $\Delta_1$ , but merely indicates that the Rabi frequency is not a good characterization of the driving pulse.

In Fig. 7, we have plotted the output Stokes intensity versus input intensity, for a fixed amplifier length, and for the detunings  $\Delta_1 = 10$  and  $\Delta_1 = 100$ . As already discussed, for a given detuning the output remains constant when the atomic medium is saturated ("linear regime"). However, before reaching this regime, the Stokes output goes through a maximum corresponding to the transition between the linear regime and the "non-linear regime" (field depleted).

The maximum output is about an order of magnitude larger for  $\Delta_1 = 100$  than for  $\Delta_1 = 10$ , although the corresponding driving energy is only about a factor of 2 larger. Thus, it is advantageous to stay away from resonance, in order to minimize the relative role of the two-photon effects. This has actually been observed. In a series of experiments, Reif and Walther chose to work extremely close to resonance, with the hope of increasing the quantum conversion efficiency of the

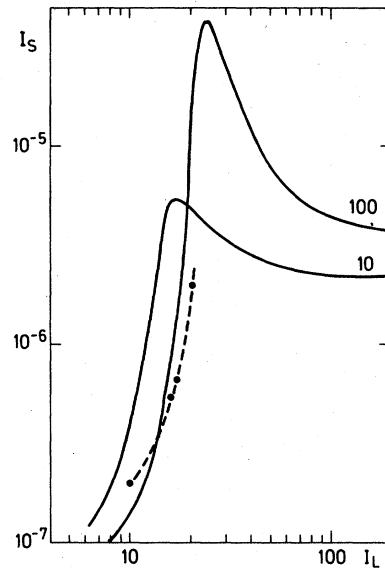


FIG. 7. Solid lines: Stokes energy versus input laser energy for a fixed amplifier length and a fixed pump duration. Same parameters as in Fig. 2, except for the detuning  $\Delta_1$ , which labels the curves. Arbitrary units. Dashed curve: experimental results of Ref. 2, arbitrary units.

system.<sup>4</sup> However, no improvement was observed as compared to experiments performed far from resonance.

The dotted curve gives the experimental points of Reif and Walther,<sup>2</sup> and they show an excellent qualitative agreement with the theoretical curve, provided that one assumes that the pump laser was significantly depleted. It is important at this point to recall that the output value of the laser was not measured. Rather, the small-signal regime was inferred on the basis of the low photon-conversion efficiency.

We have seen, however, that the nonlinear regime of hyper-Raman scattering is *not* characterized by a large Stokes field. Thus, we argue that in this experiment, the pump was significantly depleted and that the system was operated in the non-linear regime. This is confirmed by recent experiments<sup>8</sup> where the power of the input laser was increased up to the point where it has been observed that the Stokes intensity becomes independent of the pump intensity. To reach this regime, it was necessary to increase  $I_L$  by about a factor of 20. This order of magnitude is consistent with our theoretical predictions. (We note, however, that the data used in the numerical analysis are not the same as in this experiment.)

### C. Pump pulse duration

In Fig. 8, we show the growth of the Stokes field as a function of amplifier length for various

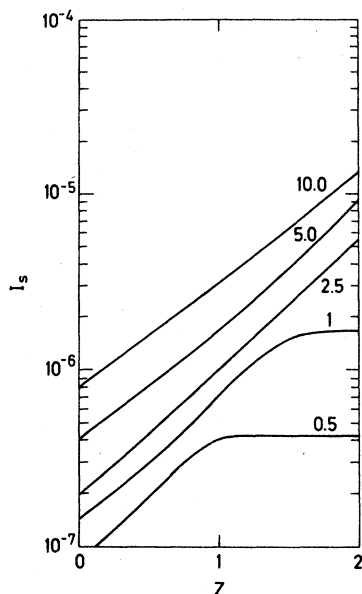


FIG. 8. Stokes energy as a function of amplifier length (arbitrary units) for various pump pulse durations, labeled on the figure. The other parameters are the same as in Fig. 2, and the peak Rabi frequency of the input laser is  $\Omega_L = 10$ .

pump fields with the same peak power but of different duration. For numerical reasons, the normalization of the initial Stokes field is different for various pulse durations, so that the origin is different for different curves. However, this is not important, since we are only interested in discussing the slopes. We see as before that except for very short  $z$ , the growth is first exponential with a rate roughly independent of the pump length. However, the saturation (pump depletion) occurs obviously earlier for smaller incident pulse duration, since there is then less energy in the pulse.

In Fig. 9, we show again the Stokes intensity as a function of amplifier length, but for a detuning  $\Delta_1 = 100$ . The solid lines are for a peak incident Rabi frequency  $\Omega_L = 12.5$ , and various pump durations. They present the same features as exhibited in Fig. 8. The dashed lines are for the same pumps and same detuning. However, the decay times of the atomic levels 2, 3, and 4 have been increased by a factor of 10. This leads to an increase of the growth rate of the Stokes field by about a factor of 3. This again illustrates the point already mentioned previously: The hyper-Raman effect is improved under conditions such that the lower order processes are weakened. Previously, this was done by either considering larger detunings, or weaker pump fields. In the case illustrated in Fig. 9, our goal is achieved by decreasing the population decay rates, thus mak-

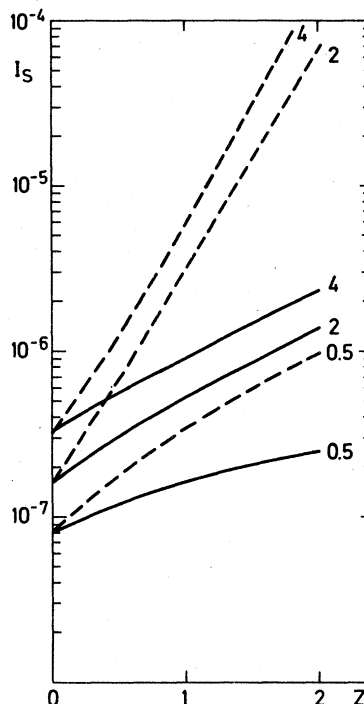


FIG. 9. Same as Fig. 8, but for a detuning  $\Delta_1 = 100$  and a peak Rabi frequency of 12.5. Solid curves:  $\gamma_{22} = \gamma_{33} = 2\gamma_{44} = 1$ . Dashed curves:  $\gamma_{22} = \gamma_{33} = 2\gamma_{44} = 0.1$ . Other parameters as in Fig. 2.

ing the system harder to saturate.

It is important, however, to note that this improvement is costly: In order to keep the same "gain" coefficients in the Maxwell equations (3.6), it is necessary to increase  $N_{\text{eff}}$  (i.e., the density of atoms) by the same factor as the lifetimes of the levels.

The statement that the hyper-Raman output is optimized if the two-photon effects are decreased should obviously be taken carefully. Clearly, the hyper-Raman effect can not appear if there are no two-photon effects going on. This is illustrated in the very weak pump-field limit, where the Stokes output becomes vanishingly small. Similarly, one does not expect the output to increase *ad eternum* for ever larger detunings. Our statement is simply that for a given atomic system, there is a range of detunings for which the output Stokes, for a given amplifier length, is optimized.<sup>5</sup> The important point is that this is *not* for  $\Delta_1 \cong 0$ . In practice, one is always limited by the available lasers and the atomic densities which can be obtained, and optimization may be hard to achieve.<sup>9</sup>

From these results, we conclude that hyper-Raman scattering in four-level-atom vapors is characterized by two main features: For small amplifier length, the atomic system is completely



saturated, and the Stokes field is weak and independent of the pump power. In the strong-signal regime (or more precisely nonlinear regime), the pump is significantly depleted, but most of its energy is lost to competing processes, and the Stokes signal remains small. (Note that this justifies *a posteriori* the neglect of the forward-backward wave coupling, even in the nonlinear regime.) The performance of the amplifier is improved by decreasing the relative role of two-photon effects, and operating between these two regimes.

#### D. Tuning range

In Fig. 10, we show the output Stokes intensity, for a fixed amplifier length and a fixed pump intensity, as a function of the detuning  $\Delta_2$ . The principal feature is that it is not symmetrical about  $\Delta_2 = 0$ . This is easy to understand, since we have to reach level 3 via a two-photon excitation. Suppose for the sake of discussion that for  $\Delta_2$  small and positive,  $\Delta_1$  is large and positive. (This is the situation encountered in the experiments of Reif and Walther.) When  $\Delta_2$  is decreased by some amount  $\epsilon$ ,  $\Delta_1$  obviously decreases by  $\epsilon/2$ . Thus, one sees that as  $\Delta_2$  goes through zero and becomes negative,  $\Delta_1$  keeps decreasing, but remains positive. That is, one goes closer to resonance with the intermediate level of the two-photon transition. There is a competing effect between one transition going further from resonance and the other one approaching resonance. This is clearly not symmetrical about  $\Delta_2 = 0$ , and therefore one should not expect a symmetric tuning curve.

At first, the fact that in the case of Fig. 8 the system delivers a higher power for positive de-

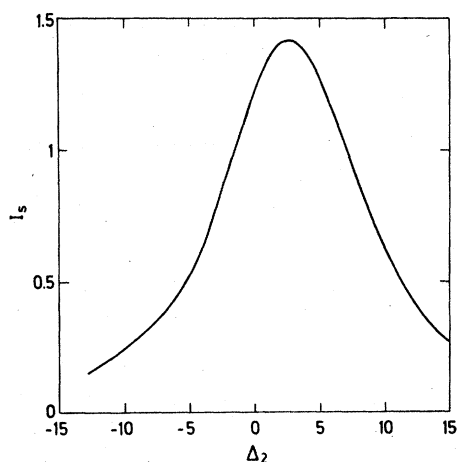


FIG. 10. Stokes energy (arbitrary units) as a function of detuning  $\Delta_2$ .  $\Delta_1$  is related to  $\Delta_2$  by the linear relation  $\Delta_1 = 9.5 + \Delta_2/2$ .

tuning  $\Delta_2$  may appear surprising, and it is in contrast with the results of Ref. 2. We attribute this feature to the fact that we have chosen numerical values such that  $\Delta_1$  becomes very small, and equals zero for  $\Delta_2 = -19$ . As the detuning  $\Delta_1$  relevant for the two-photon transition decreases, it becomes easier for the pump field to populate level 2. Thus, the pump depletion occurs over a shorter amplifier length.

This is confirmed by considering larger detunings  $\Delta_1$ . In this case, the relative change of  $\Delta_1$  for a given change of  $\Delta_2$  is much smaller, and one largely avoids effects as described above. We have considered numerically the case  $\Delta_1 \cong 40$ , and found that the peak of the tuning curve is indeed shifted toward  $\Delta_2 = 0$ . It is easy to see that in the case considered by Cotter *et al.*,<sup>3</sup> ( $\Delta_1$  large and negative), the maximum of the tuning curve should be for  $\Delta_2 < 0$ , which is also what is found experimentally.

However, for the range of parameters that we have considered, and within the numerical accuracy, we have not found a dip in the tuning curve. Reif and Walther<sup>2</sup> attributed it to the presence of other atomic levels (i.e., they do not have a real four-level system). If one supposes that the presence of these extra levels produces absorption around some wavelength near the transition 2-3, this would result in burning a hole in the tuning curve. Let us label by  $\Delta_0$  the detuning for which the tuning curve reaches its maximum. Depending upon the exact position of the extra absorption to the left or to the right of  $\Delta_2 = 0$ , one sees clearly that this can result in a tuning curve having a dip and a higher maximum to the right or the left, respectively, of  $\Delta_0$ .

#### IV. SUMMARY AND CONCLUSION

In this paper, we have shown that stimulated hyper-Raman scattering in four-level-system atomic vapors presents a number of differences from conventional Raman scattering. Because the population of the ground state is typically significantly depleted, a perturbative approach is not appropriate. Rather, it is necessary to solve the complete set of coupled density matrix and Maxwell equations.

Two regimes of interest have been found. In the linear regime, the pump field is not depleted, but the atomic medium is completely consumed by the interaction, so that the output Stokes energy is essentially independent of the pump field. In the nonlinear regime, the pump is depleted, but most of the energy deposited in the amplifier is lost to competing processes, and the Stokes energy is also very small.

The output of the system can be optimized by decreasing the relative role of laser and Raman processes, while still developing a large enough polarization to drive the Stokes wave. This can be achieved by working relatively far from resonance, and with levels having long lifetimes. Under these conditions, the transitions are harder to saturate and more energy can be transferred to the wave length of interest. We note, however, that this improvement is costly, since it implies that one has to use stronger pump lasers and/or higher atomic densities.

The essential difference between Raman and hyper-Raman scattering is that in the first case, only one interaction "channel" is normally allowed.

In this paper, we have considered perfect phase matching only. Relaxing this condition should allow for a better distinction between parametric and nonparametric processes. Because of the strong absorption at the idler frequency, however, four-wave parametric processes producing a field at  $\omega_s$  are strongly moderated even under exact phase matching. For a further discussion of this point, see Ref. 1, p. 241.

Finally, we note that we have not discussed here the spectral properties of the Stokes field. This will be the subject of a future publication.

#### ACKNOWLEDGMENTS

Numerous discussions with J. Reif and Prof. H. Walther on their experiments are gratefully acknowledged. We are thankful to Prof. C. D. Cantrell for useful discussions at the early stage of this work, and to Prof. H. Walther for bringing this problem to our attention. This work was supported by the Bundesministerium für Forschung und Technologie and Euratom. One of the authors (W.H.L.) would like to acknowledge financial support from the Humboldt Foundation and partial support by the National Science Foundation under Grant No. ENG76-23704 and by the Army Research

Office Durham under Grant No. DAAG-29-77-G-0032.

#### APPENDIX A: COMMENTS ON THE NUMERICAL SOLUTION METHOD

The neglect of backward propagation in Maxwell's equations simplifies considerably the numerical solution of the equations. Since the density matrix equations contain derivatives with respect to the retarded time  $\tau$  only, while the field equations involve only derivatives with respect to  $z'$ , it is possible to use independent steps of integration for the  $z'$  and  $\tau$  integrations. This is a standard procedure in amplifier theory. One then proceeds by integrating for all times for successive slices of amplifier.

If, as we have chosen them, the growth rates of the pump, Stokes, and idler fields are not too different, the  $z'$  integration does not present any particular difficulty. We have used a Runge-Kutta method for this part of the problem. Our major check has consisted in varying the step of integration and verifying the convergence of the output fields.

The integration of the density matrix equation is more difficult. This lies in the fact that they contain time rates of change, which can be vastly different from one another. We have found that standard integration routines were very hard to run, in particular for strong pump fields (high Rabi frequencies). For this reason, we have opted for a variable step routine<sup>10</sup> particularly adapted to stiff sets of equations. Our major check of the density matrix integration has been the conservation of its trace.

For normal runs, GEAR is as fast as standard routines. However, the integration time becomes quite large when dealing with strong fields or large detunings. Typical runs took less than 20 sec on an Amdhal 470, but the longest ones have taken up to 8 min.

\*On leave of absence from the University of Southern California.

<sup>1</sup>For a recent review, see D. C. Hanna, M. A. Yuratic, and D. Cotter, *Non-Linear Optics of Free Atoms and Molecules* (Springer, Berlin, 1979).

<sup>2</sup>J. Reif and H. Walther, *Appl. Phys.* **15**, 361 (1978). These authors call this effect hyper-Raman scattering, and in this paper, we shall use both names interchangeably. It was first observed in potassium, starting from an excited initial state, by S. Yatsiv, M. Rokni, and S. Barak, *IEEE J. Quant. Electron.* **QE-4**, 900 (1968). See also Q. H. F. Vrethen and H. M. J. Hikspoors, *Opt.*

*Commun.* **21**, 127 (1977) for experiments in a three-level system.

<sup>3</sup>D. C. Hanna, W. H. W. Tuttlebee, and M. A. Yuratic, *Opt. Commun.* **22**, 190 (1977), and Ref. 1.

<sup>4</sup>J. Reif and H. Walther (private communication, 1979).

<sup>5</sup>D. J. Kim and P. D. Coleman, *IEEE J. Quant. Electron.* **QE-16**, 300 (1980).

<sup>6</sup>C. D. Cantrell, F. A. Hopf, G. W. Rhodes, and M. O. Scully, *Appl. Opt.* **15**, 1651 (1976).

<sup>7</sup>W. H. Louisell, *Quantum Statistical Properties of Radiation* (Wiley, New York, 1973).

<sup>8</sup>J. Reif (private communication, 1980).

<sup>9</sup>This is also true theoretically for the numerical examples discussed here, we have not been able to determine for which the output reaches its optimum. The reason is that for large detunings, the calculations be-

come prohibitively expensive.

<sup>10</sup>A. C. Hindmarsh, GEAR: Ordinary Differential Equations System Solver, L. L. L. University of California document No. UCID-30001, Rev. 3 (unpublished).